hp-Adaptive Composite Discontinuous Galerkin Methods for Elliptic Eigenvalue Problems on Complicated Domains

Stefano Giani

School of Engineering and Computing Sciences, Durham University , South Road, Durham, DH1 3LE United Kingdom

Abstract

In this paper we develop the a posteriori error estimation of *hp*-adaptive discontinuous Galerkin composite finite element methods (DGFEMs) for the discretization of second-order elliptic eigenvalue problems. DGFEMs allow for the approximation of problems posed on computational domains which may contain local geometric features. The dimension of the underlying composite finite element space is independent of the number of geometric features. This is in contrast with standard finite element methods, as the minimal number of elements needed to represent the underlying domain can be very large and so the dimension of the finite element space. Computable upper bounds on the error for both eigenvalues and eigenfunctions are derived. Numerical experiments highlighting the practical application of the proposed estimators within an automatic *hp*-adaptive refinement procedure will be presented.

1 Introduction

Recently a new class of discontinuous finite elements, referred to as Discontinuous Galerkin Composite Finite Element Methods (DGCFEMs), have been developed for the numerical solution of partial differential equations, which are particularly suited to problems characterized by small details in the computational domain or micro-structures [1, 2].

DGCFEM is an extension of a previous continuous Galerkin multilevel method called Composite Finite Elements (CFEs) [3, 4, 5]. The key idea of DGCFEMs is to exploit in the discontinuous setting general shaped elements constructed aggregating standard smaller elements. Compared to the continuous setting used in CFE methods, the discontinuous setting simplifies the construction of the basis functions on the coarse aggregated mesh since no continuity has to be imposed across the edges (faces) of the coarse mesh and allowing for more general boundary conditions on the micro-structure. The *hp*–version of DGCFEMs for source problems has been presented in our recent article [1]. Moreover, an *hp*-adaptive algorithm for DGCFEMs for source problems has been presented in [2]. In this article, we extend the work presented in [2] to consider eigenvalue problems. In particular, we shall derive computable upper bounds on the errors for the eigenvalues and the eigenfunctions which are explicit in terms of the dependence on h and p. These upper bounds are based on the general techniques developed in the articles [6, 7, 8, 9]. Numerical experiments highlighting the performance of the proposed estimator within an *hp*-adaptive mesh refinement algorithm will also be presented.

Eigenvalue problems on domains with micro-structures or small geometrical features arise quite naturally in many applications like for example in response modes of composite materials and porous media and in the study of band-gap materials like photonic and phononic crystals. One of the most popular methods to solve problems with periodic micro-structures is homogenization [10, 11, 12, 13]. Homogenization describes the asymptotic behaviour of the eigenvalues and the eigenfunctions, as the scale of the micro-structure approaches zero. However, in many engineering problems the small scale is not such small to justify the use of homogenization or the micro-structure is not periodic at all, like in random media. A different approach that can deal with non-periodic structures is based on the variational multiscale approach in which the variational space is decomposed into coarse scale and fine scale [14, 15, 16]. As for the variational multiscale methods also our approach is not limited to problems with periodic micro-structures and the solutions on the coarse grid are approximated reconstructing relevant information from the small scale. In contrast with a standard finite element method that 'stores' geometrical information in the mesh, DGCFEM 'stores' on the coarse grid level the geometrical information from the fine scale in the basis functions. Moreover, within this framework, *hp*-adaptivity can be easily implemented to efficiently construct a sequence of adapted meshes and finite element spaces

where the error for the target eigenpair decays very fast. This could be definitely an advantage in applications where only a small number of eigenpairs are important and should be calculated with good accuracy.

In this article we consider the following model problem: find the eigenpairs (λ, u) such that

$$\begin{cases} -\Delta u &= \lambda\, u \qquad \text{in } \Omega, \\ \\ u &= 0 \qquad \text{on } \partial\Omega. \end{cases} \tag{1}$$

Here, Ω is a bounded, connected polyhedral domain in $\mathbb{R}^d$, $d > 1$, with boundary $\partial\Omega$; in particular, it is assumed that Ω is a 'complicated' domain, in the sense that it contains small details or micro-structures. The standard weak formulation of (1) is to find $u \in H_0^1(\Omega)$ such that

$$B(u,v) \equiv \int_\Omega \nabla u \cdot \nabla v \, d\mathbf{x} = \lambda \int_\Omega u \, v \, d\mathbf{x} \equiv \lambda \, (u,v) \qquad \forall\, v \in H_0^1(\Omega), \tag{2}$$

where the space $H_0^1(\Omega)$ is the standard space of functions with gradient in $L^2(\Omega)$ and with zero trace on $\partial\Omega$.

The outline of the paper is as follows. In Section 2 we describe how the composite finite element space is constructed for a domain with small geometric features. In Section 3 we introduce the discrete version of problem (1) and the discontinuous Galerkin method. In the following Section 4 the a posteriori analysis and the bounds on the errors are presented and in Section 5 the numerical results are presented. Finally in Section 6 some concluding remarks are collected.

2 Construction of the composite finite element spaces

In this section, we outline the construction of the underlying composite space. Such construction is a simplified version of the one used in [1].

2.1 Finite element meshes

In this section we briefly outline a general strategy to generate a hierarchy of reference and physical finite element meshes. To make the presentation

simpler, we have simplified the construction of the meshes removing the step where the nodes are moved to fit better the domain. This simplification make superfluous the introduction of the sequence of logical meshes as in [1]. Furthermore we also assume that $d = 2$, though the general approach naturally generalizes to higher–dimensional domains.

First, we need to construct a sequence of *reference* meshes $\hat{\mathcal{T}}_{h_i}$, $i = 1, \ldots, \ell$. We assume that the reference meshes are nested. Formally, we write this as follows: given $\hat{\kappa}_i \in \hat{\mathcal{T}}_{h_i}$, for some i, where $2 \leq i \leq \ell$, the parent element $\hat{\kappa}_{i-1} \in \hat{\mathcal{T}}_{h_{i-1}}$ such that $\hat{\kappa}_i \subset \hat{\kappa}_{i-1}$ is given by the mapping

$$\mathfrak{F}_{i-1}^{i}(\hat{\kappa}_i) = \hat{\kappa}_{i-1}.$$

Thereby, the mapping $\mathfrak{F}_i^{\ell} = \mathfrak{F}_i^{i+1} \circ \mathfrak{F}_{i+1}^{i+2} \circ \ldots \circ \mathfrak{F}_{\ell-1}^{\ell}$, provides the link between the parent elements on the reference mesh $\hat{\mathcal{T}}_{h_i}$, $i = 1, \ldots, \ell - 1$, with its children on the finest reference mesh $\hat{\mathcal{T}}_{h_\ell}$. More precisely, given an element $\hat{\kappa}_\ell \in \hat{\mathcal{T}}_{h_\ell}$, the parent element $\hat{\kappa}_i \in \hat{\mathcal{T}}_{h_i}$, $i = 1, \ldots, \ell - 1$, which satisfies $\hat{\kappa}_\ell \subset \hat{\kappa}_i$ is given by:

$$\mathfrak{F}_i^{\ell}(\hat{\kappa}_\ell) = \hat{\kappa}_i.$$

In order to ensure that on the constructed sequence of meshes, we proceed as follows: we define a coarse conforming shape–regular mesh $\hat{\mathcal{T}}_H = \{\hat{\kappa}\}$, consisting of standard quadrilaterals/triangles in two dimensions ($d = 2$) and tetrahedra/hexahedra when $d = 3$. We assume that $\hat{\mathcal{T}}_H$ is a non-boundary fitting mesh is the sense that it does not resolve the boundary of the computational domain Ω, but rather contains the domain Ω of the underlying problem:

$$\Omega \subset \Omega_H = \left(\bigcup_{\hat{\kappa} \in \hat{\mathcal{T}}_H} \hat{\kappa} \right)^{\circ} \quad \text{and} \quad \hat{\kappa}^{\circ} \cap \Omega \neq \emptyset \ \forall \hat{\kappa} \in \hat{\mathcal{T}}_H,$$

where, for a closed set $D \subset \mathbb{R}^d$, D° denotes the interior of D. The granularity of the finite element mesh $\hat{\mathcal{T}}_H$ can be too coarse to actually represent the underlying geometry Ω.

Algorithm 2.1 Refine Mesh

1: Set $\hat{\mathcal{T}}_{h_1} = \hat{\mathcal{T}}_H$, and the mesh counter $\ell = 1$.
2: Set $\hat{\mathcal{T}}_{h_{\ell+1}} = \emptyset$.
3: For all $\hat{\kappa} \in \hat{\mathcal{T}}_{h_\ell}$ do

1. If $\hat{\kappa} \subset \Omega$ then $\hat{\mathcal{T}}_{h_{\ell+1}} = \hat{\mathcal{T}}_{h_{\ell+1}} \bigcup \{\hat{\kappa}\}$;
2. Otherwise refine $\hat{\kappa} = \bigcup_{i=1}^{n_{\hat{\kappa}}} \hat{\kappa}_i$; here, $n_{\hat{\kappa}}$ will depend on both the type of element to be refined, and the type of refinement (isotropic/anisotropic) undertaken; for the standard red refinement of a triangular element $\hat{\kappa}$, we have that $n_{\hat{\kappa}} = 4$. For $i = 1, \ldots, n_{\hat{\kappa}}$, if $\hat{\kappa}_i \cap \Omega \neq \emptyset$ then set $\hat{\mathcal{T}}_{h_{\ell+1}} = \hat{\mathcal{T}}_{h_{\ell+1}} \bigcup \{\hat{\kappa}_i\}$.

4: If the reference mesh $\hat{\mathcal{T}}_{h_\ell}$ is sufficiently fine, in the sense that it provides a good representation of the boundary of Ω, then `STOP`. Otherwise, set $\ell = \ell + 1$, and `GOTO` 2.

Given $\hat{\mathcal{T}}_H$, we now construct a sequence of successively refined nested computational meshes using Algorithm 2.1.

We now proceed to define the sequence of physical meshes $\mathcal{T}_{h_i}$, $i = 1, \ldots, \ell$. To this end, we define the finest physical mesh $\mathcal{T}_{h_\ell}$ to be equal to the finest reference mesh $\hat{\mathcal{T}}_{h_\ell}$, i.e., $\mathcal{T}_{h_\ell} = \hat{\mathcal{T}}_{h_\ell}$. The newly created finest physical mesh $\mathcal{T}_{h_\ell}$ is a *standard* mesh upon which standard finite element methods may be applied. We may now naturally create a hierarchy of physical meshes $\{\mathcal{T}_{h_i}\}_{i=1}^{\ell}$ by simply coarsening $\mathcal{T}_{h_\ell}$. To this end, we define

$$\begin{aligned}\mathcal{T}_{h_i} \;=\; \{&\kappa : \kappa = \cup \kappa_\ell,\ \kappa_\ell \in \mathcal{T}_{h_\ell},\ \text{ which share a common parent from mesh level } i, \text{ i.e.,}\\ &\mathfrak{F}_i^\ell(\kappa_\ell)\ \text{ is identical for all members of this set}\},\end{aligned}$$

for $i = 1, \ldots, \ell - 1$. We refer to the coarsest level physical mesh $\mathcal{T}_{h_1}$ as the composite finite element (CFE) mesh. In particular, we denote this by $\mathcal{T}_{\mathtt{CFE}}$, i.e., $\mathcal{T}_{\mathtt{CFE}} = \mathcal{T}_{h_1}$. We stress that the elements $\kappa \in \mathcal{T}_{\mathtt{CFE}}$ consist of general polygons. We assume that the geometry is *complicated* in the sense that $\mathcal{T}_{h_\ell}$ is too fine to undertake computations. Instead, we wish to preform numerical simulations on the coarse composite finite element mesh $\mathcal{T}_{\mathtt{CFE}}$.

2.2 Finite element spaces

Given the meshes $\{\mathcal{T}_{h_i}\}_{i=1}^{\ell}$, we define the corresponding sequences of physical discontinuous Galerkin finite element spaces $V(\hat{\mathcal{T}}_{h_i}, \hat{\boldsymbol{p}})$ and $V(\mathcal{T}_{h_i}, \boldsymbol{p})$, $i =$

$1, \ldots, \ell$, respectively, consisting of piecewise discontinuous polynomials.

The CFE spaces are constructed based on employing the polynomial degree vector $\boldsymbol{p} = \{p_\kappa\}$. Thereby,

$$V(\mathcal{T}_{h_i}, \boldsymbol{p}) = \{u \in L^2(\Omega) : u|_\kappa \in \mathcal{P}_{p_\kappa}(\kappa)\ \forall \kappa \in \mathcal{T}_{h_i}\},$$

$i = 1, 2, \ldots, \ell$. Thereby, noting that the meshes $\{\mathcal{T}_{h_i}\}_{i=1}^{\ell}$ are nested, we deduce that $V(\mathcal{T}_{h_1}, \boldsymbol{p}) \subseteq V(\mathcal{T}_{h_2}, \boldsymbol{p}) \subseteq \ldots \subseteq V(\mathcal{T}_{h_\ell}, \boldsymbol{p})$. We now refer to $V(\mathcal{T}_{h_1}, \boldsymbol{p})$ as the composite finite element space $V(\mathcal{T}_{\mathtt{CFE}}, \boldsymbol{p})$, i.e., $V(\mathcal{T}_{\mathtt{CFE}}, \boldsymbol{p}) = V(\mathcal{T}_{h_1}, \boldsymbol{p})$.

Similarly we define

$$V(\hat{\mathcal{T}}_{h_i}, \hat{\boldsymbol{p}}) = \{u \in L^2(\Omega) : u|_{\hat{\kappa}} \in \mathcal{P}_{\hat{p}_{\hat{\kappa}}}(\hat{\kappa})\ \forall \hat{\kappa} \in \hat{\mathcal{T}}_{h_i}\},$$

for $i = 1, 2, \ldots, \ell$.

3 Composite discontinuous Galerkin finite element method

In this section, we introduce the *hp*-version of the symmetric interior penalty DGCFEM for the numerical approximation of (1). To this end, we first introduce the following notation, which is the same as in [1]. We denote by $\mathcal{F}^{\mathcal{I}}_{\mathtt{CFE}}$ the set of all interior faces of the partition $\mathcal{T}_{\mathtt{CFE}}$ of Ω, and by $\mathcal{F}^{\mathcal{B}}_{\mathtt{CFE}}$ the set of all boundary faces of $\mathcal{T}_{\mathtt{CFE}}$. Furthermore, we define $\mathcal{F} = \mathcal{F}^{\mathcal{I}}_{\mathtt{CFE}} \cup \mathcal{F}^{\mathcal{B}}_{\mathtt{CFE}}$. We emphasize that the term 'faces', of a given composite element $\kappa \in \mathcal{T}_{\mathtt{CFE}}$, consists of straight/coplanar $(d-1)$–dimensional segments of the polygonal/polyhedral domain κ. The boundary $\partial\kappa$ of an element κ and the sets $\partial\kappa \setminus \partial\Omega$ and $\partial\kappa \cap \partial\Omega$ will be identified in a natural way with the corresponding subsets of $\mathcal{F}$. Let κ^+ and κ^- be two adjacent elements of $\mathcal{T}_{\mathtt{CFE}}$, and $\mathbf{x}$ an arbitrary point on the interior face $F \in \mathcal{F}^{\mathcal{I}}_{\mathtt{CFE}}$ given by $F = \partial\kappa^+ \cap \partial\kappa^-$. Furthermore, let v and $\mathbf{q}$ be scalar- and vector-valued functions, respectively, that are smooth inside each element $\kappa^\pm$. By $(v^\pm, \mathbf{q}^\pm)$, we denote the traces of $(v, \mathbf{q})$ on F taken from within the interior of $\kappa^\pm$, respectively. Then, the averages of v and $\mathbf{q}$ at $\mathbf{x} \in F$ are given by

$$\{\!\{v\}\!\} = \frac{1}{2}(v^+ + v^-), \qquad \{\!\{\mathbf{q}\}\!\} = \frac{1}{2}(\mathbf{q}^+ + \mathbf{q}^-),$$

respectively. Similarly, the jumps of v and $\mathbf{q}$ at $\mathbf{x} \in F$ are given by

$$[\![v]\!] = v^+ \, \mathbf{n}_{\kappa^+} + v^- \, \mathbf{n}_{\kappa^-}, \qquad [\![\mathbf{q}]\!] = \mathbf{q}^+ \cdot \mathbf{n}_{\kappa^+} + \mathbf{q}^- \cdot \mathbf{n}_{\kappa^-},$$

respectively, where we denote by $\mathbf{n}_{\kappa^\pm}$ the unit outward normal vector of $\partial\kappa^\pm$, respectively. On a boundary face $F \in \mathcal{F}^{\mathcal{B}}_{\mathtt{CFE}}$, we set $\{\!\{v\}\!\} = v$, $\{\!\{\mathbf{q}\}\!\} = \mathbf{q}$, and $[\![v]\!] = v\mathbf{n}$, with $\mathbf{n}$ denoting the unit outward normal vector on the boundary $\partial\Omega$.

With this notation, we make the following key assumptions introduced in [1]:

(A1) For all elements $\kappa \in \mathcal{T}_{\mathtt{CFE}}$, we define

$$C_\kappa = \operatorname{card}\{F \in \mathcal{F} : F \subset \partial\kappa\}.$$

In the following we assume that there exists a positive constant C_F such that

$$\max_{\kappa\in\mathcal{T}_{\mathtt{CFE}}} C_\kappa \leq C_F,$$

uniformly with respect to the mesh size.

(A2) Inverse inequality. Given a face $F \in \mathcal{F}$ of an element $\kappa \in \mathcal{T}_{\mathtt{CFE}}$, there exists a positive constant C_{inv}, independent of the local mesh size and local polynomial order, such that

$$\|v\|^2_{L_2(F)} \leq C_{\mathrm{inv}} \frac{p_\kappa^2}{h_F} \|v\|^2_{L_2(\kappa)}$$

for all $v \in V(\mathcal{T}_{\mathtt{CFE}}, \boldsymbol{p})$, where h_F is a representative length scale associated to the face $F \subset \partial\kappa$.

(A3) We assume that the polynomial degree vector $\boldsymbol{p}$ is of bounded local variation, that is, there is a constant $\rho \geq 1$ such that

$$\rho^{-1} \leq p_\kappa / p_{\kappa'} \leq \rho,$$

whenever κ and κ' share a common face ($(d-1)$–dimensional facet).

The Assumption (A2) differs from the one in [1], but it is straightforward to see that it implies the one in [1] since $\nabla v \in [V(\mathcal{T}_{\mathtt{CFE}}, \boldsymbol{p})]^2$.

With this notation, we consider the (symmetric) interior penalty hp–DGCFEM for the numerical approximation of (1): find $(\lambda_{j,h}, u_{j,h}) \in \mathbb{R} \times V(\mathcal{T}_{\mathtt{CFE}}, \boldsymbol{p})$ such that

$$B_{\mathtt{DG}}(u_{j,h}, v) = \lambda_{j,h}(u_{j,h}, v) \tag{3}$$

for all $v \in V(\mathcal{T}_{\mathtt{CFE}}, \boldsymbol{p})$, where

$$B_{\mathtt{DG}}(u,v) = \sum_{\kappa\in\mathcal{T}_{\mathtt{CFE}}} \int_\kappa \nabla u \cdot \nabla v \, d\mathbf{x} - \sum_{F\in\mathcal{F}} \int_F \left(\{\!\{\nabla_h v\}\!\} \cdot [\![u]\!] + \{\!\{\nabla_h u\}\!\} \cdot [\![v]\!] \right) ds + \sum_{F\in\mathcal{F}} \int_F \sigma \, [\![u]\!] \cdot [\![v]\!] \, ds,$$

$$(u,v) = \int_\Omega u \, v \, d\mathbf{x}.$$

Here, ∇_h denotes the elementwise gradient operator. Furthermore, the function $\sigma \in L^\infty(\mathcal{F})$ is the discontinuity stabilization function that is chosen as follows: we define the function $\mathtt{p} \in L^\infty(\mathcal{F})$ by

$$\mathtt{p}(\mathbf{x}) := \begin{cases} \max(p_\kappa, p_{\kappa'}), & \mathbf{x} \in F \in \mathcal{F}^{\mathcal{I}}_{\mathtt{CFE}},\ F = \partial\kappa \cap \partial\kappa', \\ p_\kappa, & \mathbf{x} \in F \in \mathcal{F}^{\mathcal{B}}_{\mathtt{CFE}},\ F \subset \partial\kappa \cap \partial\Omega, \end{cases}$$

and set

$$\sigma|_F = \gamma \mathtt{p}^2 h_F^{-1}, \tag{4}$$

with a parameter $\gamma > 0$ that is independent of h_F and $\mathbf{p}$.

We conclude this section by equipping the composite finite element space $V(\mathcal{T}_{\mathtt{CFE}}, \boldsymbol{p})$ with the DG energy norm $|||\cdot|||_{\mathtt{DG}}$ defined by

$$|||\, v \,|||^2_{\mathtt{DG}} = \sum_{\kappa\in\mathcal{T}_{\mathtt{CFE}}} \|\nabla v\|^2_{L^2(\kappa)} + \sum_{F\in\mathcal{F}} \|\sigma^{1/2} [\![v]\!]\|^2_{L^2(F)}.$$

The stability and *a priori* error analysis of the *hp*–DGCFEM has been proven in [1] for linear problems; as for the standard symmetric interior penalty method, the discrete problem is well–posed only if γ is chosen to be sufficiently large.

4 A posteriori error analysis

In this section, we develop the *a posteriori* error analysis of the *hp*–DGCFEM defined by (3). The analysis has been inspired by [2] and [17]. The main difference between the a posteriori analysis for linear problems in [2] and the present a posteriori analysis for eigenvalue problems is the treatment of the higher order terms in the reliability results Theorem 4.2 and Corollary 4.6.

To this end, we define the distance of an approximate eigenfunction from the true eigenspace, which is a crucial quantity in the convergence analysis for eigenvalue problems especially in the case of non-simple eigenvalues.

Definition 4.1. *Given a function $v \in L^2(\Omega)$ and a finite dimensional subspace $\mathcal{P} \subset L^2(\Omega)$, we define:*

$$\operatorname{dist}(v, \mathcal{P})_{L^2(\Omega)} \;:=\; \min_{w \in \mathcal{P}} \|v - w\|_{L^2(\Omega)} \;. \tag{5}$$

Similarly, given a function $v \in S_{\underline{p}}(\mathcal{T})$ and a finite dimensional subspace $\mathcal{P} \subset H_0^1(\Omega)$, we define:

$$\operatorname{dist}(v, \mathcal{P})_{\mathtt{DG}} \;:=\; \min_{w \in \mathcal{P}} |||\, v - w \,|||_{\mathtt{DG}} \;. \tag{6}$$

Now let λ_j be any eigenvalue of problem (1) and let $M(\lambda_j)$ denote the span of all corresponding eigenfunctions, moreover let $M_1(\lambda_j) = \{u \in M(\lambda_j) : \|u\|_{L^2(\Omega)} = 1\}$.

The proof of the next result, which is one of the main results of this work, is postponed to the end of the present section.

Theorem 4.2 (Reliability for eigenfunctions)**.** *Let $(\lambda_{j,hp}, u_{j,hp})$ be a computed eigenpair of (3) converging to the true eigenvalue λ_j of multiplicity $R \geq 1$. Then we have that:*

$$\operatorname{dist}(u_{j,h}, M_1(\lambda_j))_{\mathtt{DG}} \leq C \left(\sum_{\kappa \in \mathcal{T}_{\mathtt{CFE}}} \eta_\kappa^2 \right)^{\frac{1}{2}} + \|\lambda_j u_j - \lambda_{j,h} u_{j,h}\|_{L^2(\Omega)}, \tag{7}$$

where the local error indicators η_κ, $\kappa \in \mathcal{T}_{\mathtt{CFE}}$, are defined by

$$\begin{aligned} \eta_\kappa^2 \;&=\; h_\kappa^2 p_\kappa^{-2} \|\lambda_{j,h} u_{j,h} + \Delta u_{j,h}\|_{L^2(\kappa)}^2 \\ &\quad + \sum_{F \subset \partial\kappa \setminus \partial\Omega} h_\kappa^2 h_F^{-1} p_\kappa^{-1} \|[\![\nabla u_{j,h}]\!]\|_{L^2(F)}^2 + \sigma h_\kappa^2 h_F^{-2} p_\kappa \|[\![u_{j,h}]\!]\|_{L^2(\partial\kappa)}^2 . \end{aligned} \tag{8}$$

Here, $C > 0$ is a constant that is independent of discretization parameters, and only depends on the shape-regularity of the mesh and the constants C_F, C_{inv}, and ρ from Assumptions (A1), (A2), and (A3), respectively.

The reliability for eigenvalues, Corollary 4.6, is based on the reliability for eigenfunctions, Theorem 4.2. However in the DG case the result is not as

straightforward as in the continuous Galerkin case [18]. The difficulty raises from the fact that the identity result in Lemma 4.5 holds for the extended form of the operator. To be able to introduce such form, we introduce the following lifting operator already used in [8, 19]. For any v belonging to $V(\mathcal{T}_{\mathtt{CFE}}, \boldsymbol{p}) + H^1(\Omega)$, we define $\mathcal{L}(v) \in [V(\mathcal{T}_{\mathtt{CFE}}, \boldsymbol{p})]^d$ by

$$\sum_{\kappa \in \mathcal{T}_{\mathtt{CFE}}} \int_\kappa \mathcal{L}(v) \cdot \mathbf{q} \, dx \;=\; \sum_{F \in \mathcal{F}(\mathcal{T})} \int_F [\![v]\!] \cdot \{\!\{ \mathbf{q} \}\!\} \, ds \;, \quad \forall \mathbf{q} \in V(\mathcal{T}_{\mathtt{CFE}}, \boldsymbol{p})^d \;. \tag{9}$$

Now, the following extended bilinear form $\tilde{B}_{hp}(u, v)$ can be introduced:

$$\begin{aligned} \tilde{B}_{\mathtt{DG}}(u, v) = & \sum_{\kappa \in \mathcal{T}_{\mathtt{CFE}}} \int_\kappa \nabla u \cdot \nabla v \, d\mathbf{x} - \sum_{\kappa \in \mathcal{T}_{\mathtt{CFE}}} \int_\kappa \mathcal{L}(u) \cdot \nabla v + \mathcal{L}(v) \cdot \nabla u \, d\mathbf{x} \\ & + \sum_{F \in \mathcal{F}} \int_F \sigma \, [\![u]\!] \cdot [\![v]\!] \, ds, \end{aligned} \tag{10}$$

and the corresponding discrete problem is to find $(\lambda_{j,h}, u_{j,h}) \in \mathbb{R} \times V(\mathcal{T}_{\mathtt{CFE}}, \boldsymbol{p})$ such that

$$\tilde{B}_{\mathtt{DG}}(u_{j,h}, v) = \lambda_{j,h} \, b(u_{j,h}, v), \quad \forall v \in V(\mathcal{T}_{\mathtt{CFE}}, \boldsymbol{p}). \tag{11}$$

Remark 4.3. *It is clear that $\tilde{B}_{\mathtt{DG}}(\cdot, \cdot) \equiv B_{\mathtt{DG}}(\cdot, \cdot)$ on $V(\mathcal{T}_{\mathtt{CFE}}, \boldsymbol{p}) \times V(\mathcal{T}_{\mathtt{CFE}}, \boldsymbol{p})$ and $\tilde{B}_{\mathtt{DG}}(\cdot, \cdot) \equiv B(\cdot, \cdot)$ on $H_0^1(\Omega) \times H_0^1(\Omega)$.*

It is possible to prove using [8, Lemma 4.3] and Assumption (A2) that the bilinear form $\tilde{B}_{\mathtt{DG}}(\cdot, \cdot)$ is continuous on $V(\mathcal{T}_{\mathtt{CFE}}, \boldsymbol{p}) + H^1(\Omega)$, i.e.,

$$|\tilde{B}_{\mathtt{DG}}(u, v)| \leq C_{\tilde{\mathcal{B}}} ||| \, u \, |||_{\mathtt{DG}} \; ||| \, v \, |||_{\mathtt{DG}} \;, \tag{12}$$

with a constant $C_{\tilde{\mathcal{B}}} > 0$ independent of h and p.

Definition 4.4 (Residual of a linear problem)**.** *Let define the residual for a linear problem $-\Delta u = f$, with $f \in L^2(\Omega)$, as*

$$\mathcal{R}(u, v) \;:=\; \tilde{B}_{\mathtt{DG}}(u, v) - (f, v) \;, \tag{13}$$

where $u \in H^s(\Omega)$, with $s \geq 2$, is the solution of the linear problem and $v \in V(\mathcal{T}_{\mathtt{CFE}}, \boldsymbol{p}) + H^1(\Omega)$.

We extend Definition 4.4 to the eigenvalue case allowing $f = \lambda_j u_j$, so for any eigenpair (λ_j, u_j) of problem (1):

$$\mathcal{R}(u_j, v) \;:=\; \tilde{B}_{\mathtt{DG}}(u_j, v) - \lambda_j(u_j, v)\;, \tag{14}$$

where $v \in V(\mathcal{T}_{\mathtt{CFE}}, \boldsymbol{p}) + H^1(\Omega)$.

Lemma 4.5 (Identity result for the extended form)**.** *Let (λ_l, u_l) be a true eigenpair of problem (2) with $\|u_l\|_{L^2(\Omega)} = 1$ and let $(\lambda_{j,h}, u_{j,h})$ be a computed eigenpair of problem (11) with $\|u_{j,h}\|_{L^2(\Omega)} = 1$. Then we have:*

$$\tilde{B}_{\mathtt{DG}}(u_l - u_{j,h}, u_l - u_{j,h}) \;=\; \lambda_l \|u_l - u_{j,h}\|^2_{L^2(\Omega)} \;+\; \lambda_{j,h} - \lambda_l + 2\mathcal{R}(u_l, u_j - u_{j,h}).$$

Proof. Using the linearity of the bilinear form $\tilde{B}_{\mathtt{DG}}(\cdot,\cdot)$ and using (2) and (11), we have

$$\tilde{B}_{\mathtt{DG}}(u_l - u_{j,h}, u_l - u_{j,h}) \;=\; \lambda_l + \lambda_{j,h} - 2\tilde{B}_{\mathtt{DG}}(u_l, u_{j,h}) + 2\lambda_l(u_l, u_{j,h}) - 2\lambda_l(u_l, u_{j,h})\;. \tag{15}$$

Furthermore, by analogous arguments we obtain

$$\|u_l - u_{j,h}\|^2_{L^2(\Omega)} \;=\; 2 \;-\; 2(u_l, u_{j,h}). \tag{16}$$

Substituting (16) into (15) we obtain

$$\tilde{B}_{\mathtt{DG}}(u_l - u_{j,h}, u_l - u_{j,h}) \;=\; \lambda_l \|u_l - u_{j,h}\|^2_{L^2(\Omega)} + \lambda_{j,h} - \lambda_l - 2\tilde{B}_{\mathtt{DG}}(u_l, u_{j,h}) + 2\lambda_l(u_l, u_{j,h})\;.$$

Finally, noticing that $\tilde{B}_{\mathtt{DG}}(u_l, u_j) = \lambda_l(u_l, u_j)$ and using (14) we obtain the result. □

Corollary 4.6 (Reliability for eigenvalues)**.** *Under the same assumptions of Theorem 4.2, the following hp–version a posteriori error bound holds:*

$$|\lambda_j - \lambda_{j,h}| \leq C \sum_{\kappa \in \mathcal{T}_{\mathtt{CFE}}} \eta_\kappa^2 + G\;, \tag{17}$$

where

$$G = \Big(1 + \frac{h}{p}\Big)^2 \|\lambda_j u_j - \lambda_{j,h} u_{j,h}\|^2_{L^2(\Omega)} + 2\Big(\sum_{\kappa \in \mathcal{T}_{\mathtt{CFE}}} \eta_\kappa^2\Big)^{\frac{1}{2}} \Big(1 + \frac{h}{p}\Big) \|\lambda_j u_j - \lambda_{j,h} u_{j,h}\|_{L^2(\Omega)} + 2|\mathcal{R}(\hat{u}_j, \hat{u}_j - u_{j,h})|,$$

where u_j is the minimizer of (5) and $\hat{u}_j$ is the minimizer of (6).

Proof. Applying (12) to Lemma 4.5 and also noticing that $\lambda_j\|\hat{u}_j - u_{j,hp}\|^2_{0,\Omega} > 0$ we have

$$|\lambda_j - \lambda_{j,hp}| \lesssim \mathrm{dist}(u_{j,hp}, M_1(\lambda_j))^2_{\mathtt{DG}} + 2|\mathcal{R}(\hat{u}_j, \hat{u}_j - u_{j,h})| \ .$$

Applying Theorem 4.2

$$|\lambda_j - \lambda_{j,h}| \lesssim \Big(\Big(\sum_{\kappa\in\mathcal{T}_{\mathtt{CFE}}} \eta_\kappa^2\Big)^{\frac{1}{2}} + \Big(1+\frac{h}{p}\Big)\|\lambda_j u_j - \lambda_{j,h}u_{j,h}\|_{L^2(\Omega)}\Big)^2 + 2|\mathcal{R}(\hat{u}_j, \hat{u}_j - u_{j,h})|.$$

□

4.1 Proof of Theorem 4.2

In this section we present the proof of the upper bound stated in Theorem 4.2. The proceeding proof is based on employing an *hp*–version decomposition result for the finest (reference) finite element space $V(\hat{\mathcal{T}}_{h_\ell}, \hat{\boldsymbol{p}})$, the same approach is used in [2] for linear problems. For simplicity, we assume that the finest reference mesh $\hat{\mathcal{T}}_{h_\ell}$ is conforming, i.e., it does not contain any hanging nodes. However, meshes containing hanging nodes can be admitted, based on exploiting the hierarchical construction studied in [9, 20, 21]. Writing $\mathcal{F}(\hat{\mathcal{T}}_{h_\ell})$ to denote the set of all faces of the partition $\hat{\mathcal{T}}_{h_\ell}$ of Ω, we define the discontinuity stabilization function $\hat{\sigma}$ on $\mathcal{F}(\hat{\mathcal{T}}_{h_\ell})$ by

$$\hat{\sigma} = \gamma\, \hat{\mathtt{p}}^2\, \hat{\mathtt{h}}^{-1}.$$

Here, $\hat{\mathtt{p}} \in L^\infty(\mathcal{F}(\hat{\mathcal{T}}_{h_\ell}))$ is defined in an analogous fashion to $\mathtt{p}$; indeed,

$$\hat{\mathtt{p}}(\mathbf{x}) := \begin{cases} \max(p_{\hat{\kappa}}, p_{\hat{\kappa}'}), & \mathbf{x} \in F = \partial\hat{\kappa} \cap \partial\hat{\kappa}', \\ p_{\hat{\kappa}}, & \mathbf{x} \in F \subset \partial\hat{\kappa} \cap \partial\Omega. \end{cases}$$

Similarly, $\hat{\mathtt{h}} \in L^\infty(\mathcal{F}(\hat{\mathcal{T}}_{h_\ell}))$ is given by

$$\hat{\mathtt{h}}(\mathbf{x}) := \begin{cases} \min(h_{\hat{\kappa}}, h_{\hat{\kappa}'}), & \mathbf{x} \in \ F = \partial\hat{\kappa} \cap \partial\hat{\kappa}', \\ h_{\hat{\kappa}}, & \mathbf{x} \in \ F \subset \partial\hat{\kappa} \cap \partial\Omega. \end{cases}$$

Furthermore, on $\hat{\mathcal{T}}_{h_\ell}$, we define the norm

$$|||\, v\, |||^2_{\widehat{\mathtt{DG}}} = \sum_{\kappa\in\hat{\mathcal{T}}_{h_\ell}} \|\nabla v\|^2_{L^2(\kappa)} + \sum_{F\in\mathcal{F}(\hat{\mathcal{T}}_{h_\ell})} \|\hat{\sigma}^{1/2}[\![v]\!]\|^2_{L^2(F)}.$$

We write $V^c(\hat{\mathcal{T}}_{h_\ell}, \hat{\boldsymbol{p}}) = V(\hat{\mathcal{T}}_{h_\ell}, \hat{\boldsymbol{p}}) \cap H_0^1(\Omega)$. The orthogonal complement of $V^c(\hat{\mathcal{T}}_{h_\ell}, \hat{\boldsymbol{p}})$ in $V(\hat{\mathcal{T}}_{h_\ell}, \hat{\boldsymbol{p}})$ with respect to the norm $|||\cdot|||_{\widehat{\mathtt{DG}}}$ is denoted by $V^\perp(\hat{\mathcal{T}}_{h_\ell}, \hat{\boldsymbol{p}})$, such that

$$V(\hat{\mathcal{T}}_{h_\ell}, \hat{\boldsymbol{p}}) = V^c(\hat{\mathcal{T}}_{h_\ell}, \hat{\boldsymbol{p}}) \oplus V^\perp(\hat{\mathcal{T}}_{h_\ell}, \hat{\boldsymbol{p}}).$$

With this notation in mind, we recall the following four results published in [2].

Proposition 4.7. *There is an approximant $\mathcal{A} : V(\hat{\mathcal{T}}_{h_\ell}, \hat{\boldsymbol{p}}) \to V^c(\hat{\mathcal{T}}_{h_\ell}, \hat{\boldsymbol{p}})$ that satisfies*

$$\|\nabla_h(v - \mathcal{A}v)\|^2_{L^2(\Omega)} \leq C \sum_{F \in \mathcal{F}(\hat{\mathcal{T}}_{h_\ell})} \int_F \hat{\mathtt{p}}^2 \hat{\mathtt{h}}^{-1} |[\![v]\!]|^2 \, ds, \qquad v \in V(\hat{\mathcal{T}}_{h_\ell}, \hat{\boldsymbol{p}}),$$

with a constant $C > 0$ that is independent of the mesh size and polynomial degrees.

Since $V(\mathcal{T}_{\mathtt{CFE}}, \boldsymbol{p}) \subseteq V(\hat{\mathcal{T}}_{h_\ell}, \hat{\boldsymbol{p}})$, the DG-solution $u_{j,h} \in V(\mathcal{T}_{\mathtt{CFE}}, \boldsymbol{p})$ obtained by (3) may be split accordingly,

$$u_{j,h} = u^c_{j,h} + u^\perp_{j,h}, \tag{18}$$

where $u^c_{j,h} \in V^c(\hat{\mathcal{T}}_{h_\ell}, \hat{\boldsymbol{p}})$ and $u^\perp_{j,h} \in V^\perp(\hat{\mathcal{T}}_{h_\ell}, \hat{\boldsymbol{p}})$. Furthermore, we define the error of the *hp*–DGCFEM by

$$e_h = u_j - u_{j,h} \equiv e^c_h - u^\perp_{j,h}, \tag{19}$$

where

$$e^c_h = u_j - u^c_{j,h} \in H_0^1(\Omega). \tag{20}$$

Proposition 4.8. *With $u^\perp_{j,h}$ and e^c_h defined by* (18) *and* (19)*, respectively, the following bounds hold:*

$$\|\nabla_h u^\perp_{j,h}\|_{L^2(\Omega)} \leq C \left(\sum_{F \in \mathcal{F}(\mathcal{T}_{\mathtt{CFE}})} \int_F \mathtt{p}^2 h_F^{-1} |[\![v]\!]|^2 \, ds \right)^{1/2}, \qquad \|\nabla e^c_h\|_{L^2(\Omega)} \leq C |||\, e_h \,|||_{\mathtt{DG}},$$

where C is a positive constant which is independent of the discretization parameters.

For the next result we use the notation, given $\kappa \in \mathcal{T}_{\mathtt{CFE}}$, we write $\hat{\kappa} \in \hat{\mathcal{T}}_{h_1}$ to denote the element in the reference mesh $\hat{\mathcal{T}}_{h_1}$ such that $\kappa \subseteq \hat{\kappa}$.

Lemma 4.9. *Given $v|_{\hat{\kappa}} \in H^1(\hat{\kappa})$, for $\hat{\kappa} \in \hat{\mathcal{T}}_{h_1}$, there exists $\hat{\mathcal{I}}v$ in $\mathcal{P}_{p_{\hat{\kappa}}}(\hat{\kappa})$, $p_{\hat{\kappa}} = 1, 2, \ldots,$ such that*

$$h_{\hat{\kappa}}^{-1} p_{\hat{\kappa}} \|v - \hat{\mathcal{I}}v\|_{L^2(\hat{\kappa})} + \|\nabla(v - \hat{\mathcal{I}}v)\|_{L^2(\hat{\kappa})} \leq C \|\nabla v\|_{L^2(\hat{\kappa})},$$

where C is a positive constant, which is independent of the local mesh size $h_{\hat{\kappa}}$ and the local polynomial degree $p_{\hat{\kappa}}$.

Then we introduce the projection operator $\mathcal{I}$ on κ by the relation

$$\mathcal{I}v = \hat{\mathcal{I}}(\mathfrak{E}v)|_{\kappa}, \tag{21}$$

where $\mathfrak{E}$ denotes the extension operator defined in [2, Theorem 2.1].

Lemma 4.10. *Given $\kappa \in \mathcal{T}_{\mathtt{CFE}}$, let $F \subset \partial\kappa$ denote one of its faces. For a function $v \in H^1(\kappa)$, the following bound holds*

$$h_{\kappa}^{-1} p_{\kappa} \|v - \mathcal{I}v\|_{L^2(\kappa)} + \|\nabla(v - \mathcal{I}v)\|_{L^2(\kappa)} + h_F^{1/2} h_{\kappa}^{-1} p_{\kappa}^{1/2} \|v - \mathcal{I}v\|_{L^2(F)} \;\leq\; C \|\nabla \mathfrak{E}v\|_{L^2(\hat{\kappa})},$$

where $p_{\kappa} \geq 1$ and C is a positive constant, independent of v and the discretization parameters.

The first step in the proof of Theorem 4.2 is to exploit the decomposition (19):

$$\begin{aligned} |||\, e_h \,|||_{\mathtt{DG}}^2 &= \sum_{\kappa \in \mathcal{T}_{\mathtt{CFE}}} \|\nabla e_h\|_{L^2(\kappa)}^2 + \sum_{F \in \mathcal{F}(\mathcal{T}_{\mathtt{CFE}})} \|\sigma^{1/2} [\![e_h]\!]\|_{L^2(F)}^2 \\ &= \sum_{\kappa \in \mathcal{T}_{\mathtt{CFE}}} \int_{\kappa} \nabla e_h \cdot \nabla e_h^c d\mathbf{x} - \sum_{\kappa \in \mathcal{T}_{\mathtt{CFE}}} \int_{\kappa} \nabla e_h \cdot \nabla u_{j,h}^{\perp} d\mathbf{x} + \sum_{F \in \mathcal{F}(\mathcal{T}_{\mathtt{CFE}})} \int_F \sigma |[\![e_h]\!]|^2 ds \\ &\equiv \mathrm{T}_1 + \mathrm{T}_2 + \mathrm{T}_3. \end{aligned} \tag{22}$$

Next, the three terms T_1, T_2, and T_3 are bounded individually.

Term T_1 Applying integration by parts we have

$$\begin{aligned}
\mathrm{T}_1 &= -\sum_{\kappa\in\mathcal{T}_{\mathtt{CFE}}}\int_\kappa \Delta u_j\, e_h^c d\mathbf{x} - \sum_{\kappa\in\mathcal{T}_{\mathtt{CFE}}}\int_\kappa \nabla u_{j,h}\cdot\nabla e_h^c d\mathbf{x} \\
&= \sum_{\kappa\in\mathcal{T}_{\mathtt{CFE}}}\int_\kappa \lambda_j u_j\, e_h^c d\mathbf{x} - \sum_{\kappa\in\mathcal{T}_{\mathtt{CFE}}}\int_\kappa \nabla u_{j,h}\cdot\nabla e_h^c d\mathbf{x} \\
&= \sum_{\kappa\in\mathcal{T}_{\mathtt{CFE}}}\int_\kappa (\lambda_j u_j - \lambda_{j,h}u_{j,h})\, e_h^c d\mathbf{x} + \sum_{\kappa\in\mathcal{T}_{\mathtt{CFE}}}\int_\kappa \lambda_{j,h}u_{j,h}\, e_h^c d\mathbf{x} - \sum_{\kappa\in\mathcal{T}_{\mathtt{CFE}}}\int_\kappa \nabla u_{j,h}\cdot\nabla e_h^c d\mathbf{x}.
\end{aligned}$$

Denoting with $\mathcal{I}e_h^c \in V(\mathcal{T}_{\mathtt{CFE}}, \boldsymbol{p})$ the element-wise interpolant of e_h^c defined by (21) and exploiting both (3) and integrating by parts elementwise, we get

$$\begin{aligned}
\mathrm{T}_1 &= \sum_{\kappa\in\mathcal{T}_{\mathtt{CFE}}}\int_\kappa (\lambda_j u_j - \lambda_{j,h}u_{j,h})\,(e_h^c - \mathcal{I}e_h^c) d\mathbf{x} + \sum_{\kappa\in\mathcal{T}_{\mathtt{CFE}}}\int_\kappa (\lambda_j u_j - \lambda_{j,h}u_{j,h})\,\mathcal{I}e_h^c d\mathbf{x} \\
&\quad + \sum_{\kappa\in\mathcal{T}_{\mathtt{CFE}}}\int_\kappa \lambda_{j,h}u_{j,h}\,(e_h^c - \mathcal{I}e_h^c) d\mathbf{x} - \sum_{\kappa\in\mathcal{T}_{\mathtt{CFE}}}\int_\kappa \nabla u_{j,h}\cdot\nabla(e_h^c - \mathcal{I}e_h^c) d\mathbf{x} \\
&\quad - \sum_{F\in\mathcal{F}(\mathcal{T}_{\mathtt{CFE}})}\int_F \left(\{\!\{\nabla_h u_{j,h}\}\!\}\cdot[\![\mathcal{I}e_h^c]\!] + \{\!\{\nabla_h \mathcal{I}e_h^c\}\!\}\cdot[\![u_{j,h}]\!]\right) ds \\
&\quad + \sum_{F\in\mathcal{F}(\mathcal{T}_{\mathtt{CFE}})}\int_F \sigma\,[\![u_{j,h}]\!]\cdot[\![\mathcal{I}e_h^c]\!]\, ds \\
&= \sum_{\kappa\in\mathcal{T}_{\mathtt{CFE}}}\int_\kappa (\lambda_j u_j - \lambda_{j,h}u_{j,h})\,(e_h^c - \mathcal{I}e_h^c) d\mathbf{x} + \sum_{\kappa\in\mathcal{T}_{\mathtt{CFE}}}\int_\kappa (\lambda_j u_j - \lambda_{j,h}u_{j,h})\,\mathcal{I}e_h^c d\mathbf{x} \\
&\quad + \sum_{\kappa\in\mathcal{T}_{\mathtt{CFE}}}\int_\kappa (\lambda_{j,h}u_{j,h} + \Delta u_{j,h})\,(e_h^c - \mathcal{I}e_h^c) d\mathbf{x} - \sum_{\kappa\in\mathcal{T}_{\mathtt{CFE}}}\int_{\partial\kappa} \frac{\partial u_{j,h}}{\partial \mathbf{n}_\kappa}(e_h^c - \mathcal{I}e_h^c) ds \\
&\quad - \sum_{F\in\mathcal{F}(\mathcal{T}_{\mathtt{CFE}})}\int_F \left(\{\!\{\nabla_h u_{j,h}\}\!\}\cdot[\![\mathcal{I}e_h^c]\!] + \{\!\{\nabla_h \mathcal{I}e_h^c\}\!\}\cdot[\![u_{j,h}]\!]\right) ds \\
&\quad + \sum_{F\in\mathcal{F}(\mathcal{T}_{\mathtt{CFE}})}\int_F \sigma\,[\![u_{j,h}]\!]\cdot[\![\mathcal{I}e_h^c]\!]\, ds.
\end{aligned}$$

We now treat the first two terms; applying Lemma 4.10 we obtain from

the first term:

$$\sum_{\kappa\in\mathcal{T}_{\texttt{CFE}}}\int_{\kappa}(\lambda_j u_j-\lambda_{j,h}u_{j,h})\,(e_h^c-\mathcal{I}e_h^c)d\mathbf{x}\leq C\left(\sum_{\kappa\in\mathcal{T}_{\texttt{CFE}}}h_\kappa^2 p_\kappa^{-2}\|\lambda_j u_j-\lambda_{j,h}u_{j,h}\|^2_{L^2(\kappa)}\right)^{1/2}\|\nabla\mathfrak{E}e_h^c\|_{L^2(\Omega_H)}\,. \tag{23}$$

To treat the second term we use the following auxiliary result which comes straightforwardly from Lemma 4.10 and the Poincaré inequality:

$$\begin{aligned}\|\mathcal{I}e_h^c\|_{L^2(\Omega)} &\leq C\frac{\max_{\kappa\in\mathcal{T}_{\texttt{CFE}}}h_\kappa}{\min_{\kappa\in\mathcal{T}_{\texttt{CFE}}}p_\kappa}\|\nabla\mathfrak{E}e_h^c\|_{L^2(\Omega_H)}+\|e_h^c\|_{L^2(\Omega)}\\ &\leq C'(\|\nabla\mathfrak{E}e_h^c\|_{L^2(\Omega_H)}+\|\nabla\mathfrak{E}e_h^c\|_{L^2(\Omega)})\leq C''\|\nabla\mathfrak{E}e_h^c\|_{L^2(\Omega_H)}\end{aligned}$$

Such result leads to:

$$\sum_{\kappa\in\mathcal{T}_{\texttt{CFE}}}\int_{\kappa}(\lambda_j u_j-\lambda_{j,h}u_{j,h})\,\mathcal{I}e_h^c d\mathbf{x}\leq C''\left(\sum_{\kappa\in\mathcal{T}_{\texttt{CFE}}}\|\lambda_j u_j-\lambda_{j,h}u_{j,h}\|^2_{L^2(\kappa)}\right)^{1/2}\|\nabla\mathfrak{E}e_h^c\|_{L^2(\Omega_H)}\,. \tag{24}$$

Putting together (23) and (24) we obtain:

$$\begin{aligned}\sum_{\kappa\in\mathcal{T}_{\texttt{CFE}}}\int_{\kappa}(\lambda_j u_j-\lambda_{j,h}u_{j,h})\,(e_h^c-\mathcal{I}e_h^c)d\mathbf{x} &+\sum_{\kappa\in\mathcal{T}_{\texttt{CFE}}}\int_{\kappa}(\lambda_j u_j-\lambda_{j,h}u_{j,h})\,\mathcal{I}e_h^c d\mathbf{x}\\ &\leq\tilde{C}\left(\sum_{\kappa\in\mathcal{T}_{\texttt{CFE}}}\|\lambda_j u_j-\lambda_{j,h}u_{j,h}\|^2_{L^2(\kappa)}\right)^{1/2}\|\nabla\mathfrak{E}e_h^c\|_{L^2(\Omega_H)}\,.\end{aligned} \tag{25}$$

We now recall the following result from [22] used to transfer between element-based and face-based integrations:

$$\begin{aligned}\sum_{\kappa\in\mathcal{T}_{\texttt{CFE}}}\int_{\partial\kappa}\frac{\partial u_{j,h}}{\partial\mathbf{n}_\kappa}(e_h^c-\mathcal{I}e_h^c)ds &= \sum_{F\in\mathcal{F}(\mathcal{T}_{\texttt{CFE}})}\int_F\{\!\{\nabla_h u_{j,h}\}\!\}\cdot[\![e_h^c-\mathcal{I}e_h^c]\!]\,ds\\ &\quad+\sum_{F\in\mathcal{F}^{\mathcal{I}}(\mathcal{T}_{\texttt{CFE}})}\int_F[\![\nabla_h u_{j,h}]\!]\{\!\{e_h^c-\mathcal{I}e_h^c\}\!\}\,ds\end{aligned} \tag{26}$$

Recalling that $e_h^c\in H_0^1(\Omega)$, it follows that $[\![e_h^c]\!]_F=\mathbf{0}$ for all $F\in\mathcal{F}(\mathcal{T}_{\texttt{CFE}})$.

Thereby,

$$\begin{aligned}
&\sum_{\kappa\in\mathcal{T}_{\texttt{CFE}}}\int_{\kappa}(\lambda_{j,h}u_{j,h}+\Delta u_{j,h})\,(e_h^c-\mathcal{I}e_h^c)d\mathbf{x}-\sum_{F\in\mathcal{F}^{\mathcal{I}}(\mathcal{T}_{\texttt{CFE}})}\int_F[\![\nabla u_{j,h}]\!]\{\!\{e_h^c-\mathcal{I}e_h^c\}\!\}\,ds\\
&\quad-\sum_{F\in\mathcal{F}(\mathcal{T}_{\texttt{CFE}})}\int_F\{\!\{\nabla_h\mathcal{I}e_h^c\}\!\}\cdot[\![u_{j,h}]\!]\,ds+\sum_{F\in\mathcal{F}(\mathcal{T}_{\texttt{CFE}})}\int_F\sigma\,[\![u_{j,h}]\!]\cdot[\![\mathcal{I}e_h^c]\!]\,ds\\
\equiv\;&\mathrm{T}_{11}+\mathrm{T}_{12}+\mathrm{T}_{13}+\mathrm{T}_{14}.
\end{aligned}\tag{27}$$

Employing the Cauchy–Schwarz inequality, together with the approximation result stated in Lemma 4.10 gives

$$\begin{aligned}
\mathrm{T}_{11}\;&\leq\;\left(\sum_{\kappa\in\mathcal{T}_{\texttt{CFE}}}h_\kappa^2p_\kappa^{-2}\|\lambda_{j,h}u_{j,h}+\Delta u_{j,h})\|_{L^2(\kappa)}^2\right)^{1/2}\left(\sum_{\kappa\in\mathcal{T}_{\texttt{CFE}}}h_\kappa^{-2}p_\kappa^2\|e_h^c-\mathcal{I}e_h^c\|_{L^2(\kappa)}^2\right)^{1/2}\\
&\leq\;C\left(\sum_{\kappa\in\mathcal{T}_{\texttt{CFE}}}h_\kappa^2p_\kappa^{-2}\|\lambda_{j,h}u_{j,h}+\Delta u_{j,h}\|_{L^2(\kappa)}^2\right)^{1/2}\|\nabla\mathfrak{E}e_h^c\|_{L^2(\Omega_H)}.
\end{aligned}\tag{28}$$

The terms T_{12}, T_{13} and T_{14} are bounded in the same way as in [2]. For brevity we report only the final results

$$\mathrm{T}_{12}\;\leq\;C\left(\sum_{\kappa\in\mathcal{T}_{\texttt{CFE}}}\sum_{F\subset\partial\kappa\setminus\partial\Omega}h_\kappa^2h_F^{-1}p_\kappa^{-1}\|[\![\nabla u_{j,h}]\!]\|_{L^2(F)}^2\right)^{1/2}\|\nabla\mathfrak{E}e_h^c\|_{L^2(\Omega_H)},\tag{29}$$

$$\mathrm{T}_{13}\leq C\left(\sum_{F\in\mathcal{F}(\mathcal{T}_{\texttt{CFE}})}\sigma\|[\![u_{j,h}]\!]\|_{L^2(F)}^2\right)^{1/2}\left(\|\nabla\mathfrak{E}e_h^c\|_{L^2(\Omega_H)}+\|\nabla e_h^c\|_{L^2(\Omega)}\right),\tag{30}$$

$$\mathrm{T}_{14}\;\leq\;C\left(\sum_{F\in\mathcal{F}(\mathcal{T}_{\texttt{CFE}})}\sigma h_\kappa^2h_F^{-2}\mathfrak{p}\|[\![u_{j,h}]\!]\|_{L^2(F)}^2\right)^{1/2}\|\nabla\mathfrak{E}e_h^c\|_{L^2(\Omega_H)}.\tag{31}$$

Substituting the bounds (25) and (28)–(31) into (27) and exploiting the ex-

tension operator [2, Theorem 2.1], we deduce that

$$\begin{aligned}
\mathrm{T}_1 \;\leq\; C \Bigg[& \left(\sum_{\kappa \in \mathcal{T}_{\mathtt{CFE}}} h_\kappa^2 p_\kappa^{-2} \|\lambda_{j,h} u_{j,h} + \Delta u_{j,h})\|_{L^2(\kappa)}^2 \right)^{1/2} \\
& + \left(\sum_{\kappa \in \mathcal{T}_{\mathtt{CFE}}} \sum_{F \subset \partial\kappa \setminus \partial\Omega} h_\kappa^2 h_F^{-1} p_\kappa^{-1} \|[\![\nabla u_{j,h}]\!]\|_{L^2(F)}^2 \right)^{1/2} \\
& + \left(\sum_{F \in \mathcal{F}(\mathcal{T}_{\mathtt{CFE}})} \sigma h_\kappa^2 h_F^{-2} \mathtt{p} \|[\![u_{j,h}]\!]\|_{L^2(F)}^2 \right)^{1/2} \\
& + \left(\sum_{\kappa \in \mathcal{T}_{\mathtt{CFE}}} \|\lambda u - \lambda_{j,h} u_{j,h}\|_{L^2(\kappa)}^2 \right)^{1/2} \Bigg] \, \|\nabla e_h^c\|_{L^2(\Omega)}.
\end{aligned}$$

Thereby, employing the Cauchy–Schwarz inequality and Proposition 4.8, gives

$$\mathrm{T}_1 \;\leq\; C \left[\left(\sum_{\kappa \in \mathcal{T}_{\mathtt{CFE}}} \eta_\kappa^2 \right)^{1/2} + \|\lambda_j u_j - \lambda_{j,h} u_{j,h}\|_{L^2(\Omega)} \right] |||\, e_h \,|||_{\mathtt{DG}}. \tag{32}$$

Term T_2 As above, employing the Cauchy–Schwarz inequality, together with Proposition 4.8, we get

$$\mathrm{T}_2 \leq \|\nabla e_h\|_{L^2(\Omega)} \|\nabla u_{j,h}^{\perp}\|_{L^2(\Omega)} \leq C \left(\sum_{\kappa \in \mathcal{T}_{\mathtt{CFE}}} \eta_\kappa^2 \right)^{1/2} |||\, e_h \,|||_{\mathtt{DG}}. \tag{33}$$

Term T_3 Noting that $u_j \in H_0^1(\Omega)$ gives

$$\mathrm{T}_3 = \sum_{F \in \mathcal{F}(\mathcal{T}_{\mathtt{CFE}})} \int_F \sigma [\![e_h]\!] \cdot [\![u_{j,h}]\!] ds \leq \left(\sum_{\kappa \in \mathcal{T}_{\mathtt{CFE}}} \eta_\kappa^2 \right)^{1/2} |||\, e_h \,|||_{\mathtt{DG}}. \tag{34}$$

Inserting the bounds (32), (33), and (34) into (22) and dividing both sides by $|||\, e_h \,|||_{\mathtt{DG}}$ completes the proof of Theorem 4.2.

5 Numerical experiments

In this section we present a series of computational examples to highlight the practical performance of the a posteriori error bounds derived in Theorem 4.2 and Corollary 4.6 for problems where the underlying computational domain contains micro-structures. Throughout this section the DGCFEM eigenpair $(\lambda_{j,h}, u_{j,h})$ defined by (3) is computed with the constant γ appearing in the discontinuity stabilization function σ equal to 10. All the numerical examples presented in this section have been computed using the AptoFEM package (`www.aptofem.com`) and the resulting generalised eigenvalue problem is solved employing ARPACK [23] and the Multifrontal Massively Parallel Solver (MUMPS) [24, 25, 26].

Algorithm 5.1 Adaptive Refinement Algorithm

1: Input parameters: refinement fraction θ_r; termination tolerance tol; maximum number of refinement steps $k_{\texttt{max}}$.
2: Initial step: Input initial composite finite element mesh $\mathcal{T}_{\texttt{CFE}}$ and reference mesh $\hat{\mathcal{T}}_{h_\ell}$, cf. Algorithm 2.1, and select initial polynomial degree distribution $\boldsymbol{p}$ in order to construct the composite and reference finite element spaces $V(\mathcal{T}_{\texttt{CFE}}, \boldsymbol{p})$ and $V(\hat{\mathcal{T}}_{h_\ell}, \hat{\boldsymbol{p}})$, respectively.
3: Set $V(\mathcal{T}_{\texttt{CFE}_1}, \boldsymbol{p}_1) = V(\mathcal{T}_{\texttt{CFE}}, \boldsymbol{p})$ and the mesh counter $k = 1$.
4: **while** $k < k_{\texttt{max}}$ **do**
5: Compute $(\lambda_{j,h}, u_{j,h}) \in \mathbb{R} \times V(\mathcal{T}_{\texttt{CFE}_k}, \boldsymbol{p}_k)$, cf. (3).
6: Evaluate the error indicators η_κ, defined by (8), for all $\kappa \in \mathcal{T}_k$
7: **if** $C \left(\sum_{\kappa \in \mathcal{T}_{\texttt{CFE}_k}} \eta_\kappa^2 \right)^{1/2} <$ tol **then**
8: Exit.
9: **else**
10: Mark elements for refinement employing the fixed fraction refinement strategy with refinement fraction θ_r.
11: **if** Element κ is marked for refinement **then**
12: Perform hp–refinement based on testing the smoothness of the computed eigenfunction $u_{j,h}$; see, e.g., [27, 28].
13: **end if**
14: Set $k = k+1$ and generate the new composite finite element space $V(\mathcal{T}_{\texttt{CFE}_k}, \boldsymbol{p}_k)$.
15: hp–Refine the reference finite element space $V(\hat{\mathcal{T}}_{h_\ell}, \hat{\boldsymbol{p}})$ (if necessary), to ensure that the inclusion $V(\mathcal{T}_{\texttt{CFE}_k}, \boldsymbol{p}_k) \subseteq V(\hat{\mathcal{T}}_{h_\ell}, \hat{\boldsymbol{p}})$ holds.
16: **end if**
17: **end while**

Algorithm 5.1 outlines the general adaptive algorithm employed within this section. In particular, we point out that the elements are marked for refinement, according to the size of the local error indicators η_κ, based on employing the fixed fraction refinement strategy; here, we set the refinement fraction θ_r, equal to 15%. Once an element $\kappa \in \mathcal{T}_{\texttt{CFE}}$ has been marked for refinement, we employ the hp–adaptive strategy developed in [27] to decide whether h– or p–refinement should be performed on κ; for related work, we refer to [28, 29], for example, and the review article [30]. Finally, we remark that to ensure that the inclusion $V(\mathcal{T}_{\texttt{CFE}_k}, \boldsymbol{p}_k) \subseteq V(\hat{\mathcal{T}}_{h_\ell}, \hat{\boldsymbol{p}})$ remains valid as the adaptive algorithm proceeds, subsequent refinement of the (finest) reference

finite element space $V(\hat{\mathcal{T}}_{h_\ell}, \hat{\boldsymbol{p}})$ may need to be undertaken. Indeed, additional refinement is performed to ensure that the following two conditions hold:

1. Given any element $\kappa \in \mathcal{T}_{\texttt{CFE}}$, we may write $\kappa = \cup \kappa_\ell$, $\kappa_\ell \in \mathcal{S}_\kappa$, where $\mathcal{S}_\kappa$ denotes a subset of elements which belong to $\hat{\mathcal{T}}_{h_\ell}$.

2. Given $\kappa \in \mathcal{T}_{\texttt{CFE}}$ and the corresponding set $\mathcal{S}_\kappa = \{\hat{\kappa} \in \hat{\mathcal{T}}_{h_\ell} : \ \hat{\kappa} \subset \kappa\}$ consisting of fine level reference elements which form κ, we require that the polynomial degree $p_{\hat{\kappa}}$ defined for each $\hat{\kappa} \in \mathcal{S}_\kappa$ is set equal to the polynomial degree p_κ of the composite element κ, i.e., $p_{\hat{\kappa}} = p_\kappa$ for all $\hat{\kappa} \in \mathcal{S}_\kappa$.

5.1 Example 1: Few holes

In this first example, we consider a unit square domain with four small square holes of size 1/32, see Figure 1. The initial coarse mesh contains only 8 triangles and the initial value of $p = 2$ for all elements.

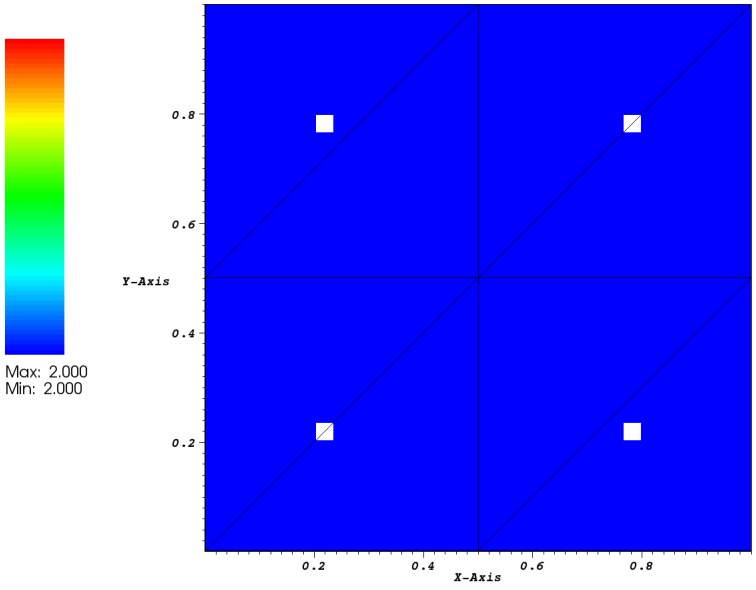

Figure 1: Example 1: Initial coarse mesh for the domain with four small holes. The color scheme indicate the order of polynomials used in each element.

In Figure 2, we present the decay of the error for the first two distinct eigenvalues and the corresponding error estimators. As can be seen the convergence for all eigenvalues look asymptotically exponential and the error estimator $\sum_{\kappa\in\mathcal{T}_{\mathtt{CFE}}}\eta_\kappa^2$ follows well the error. In Figure 3, we reported the values of the efficiency index $\sum_{\kappa\in\mathcal{T}_{\mathtt{CFE}}}\eta_\kappa^2/|\lambda_j-\lambda_{j,h}|$ for all the considered eigenvalues.

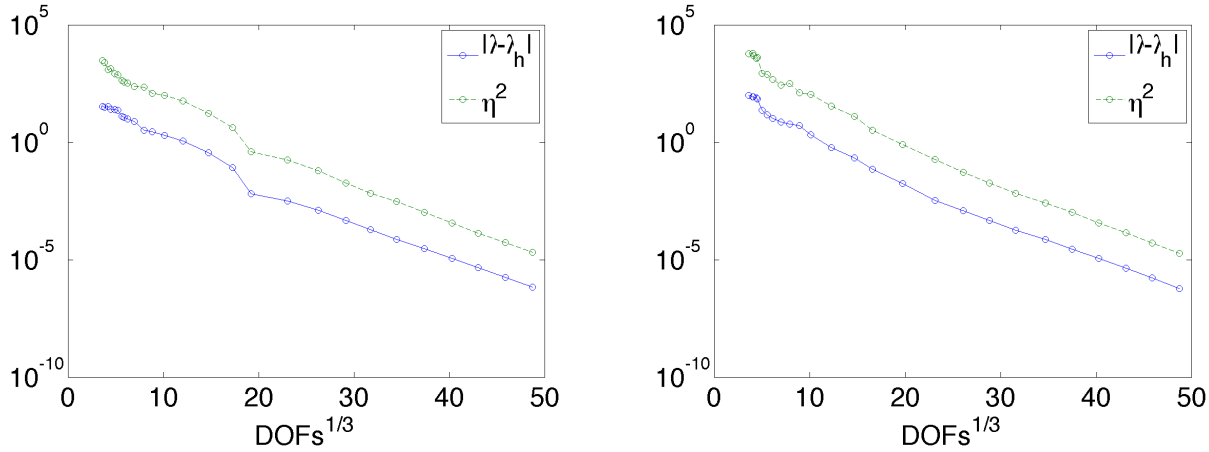

Figure 2: Example 1: (a) Convergence of the error for the first eigenvalue and of the corresponding error estimator. (b) Convergence of the error for the second eigenvalue and of the corresponding error estimator.

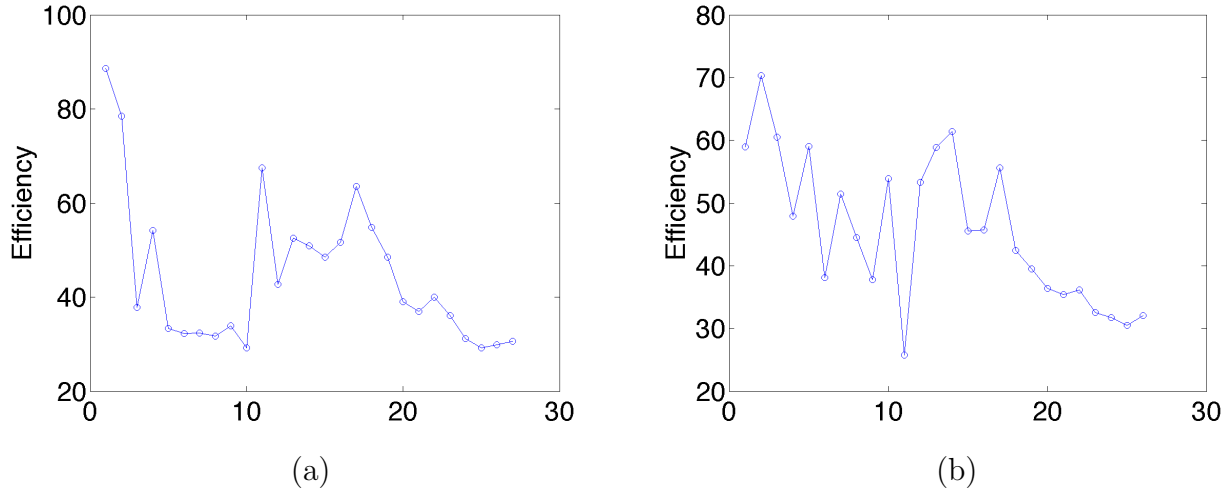

Figure 3: Example 1: (a) Efficiency index for the first eigenvalue. (b) Efficiency index for the second eigenvalue.

To have an idea of the shape of the eigenfunctions for this problem, in

Figure 4 we reported the pictures of eigenfunctions corresponding to the first two eigenvalues.

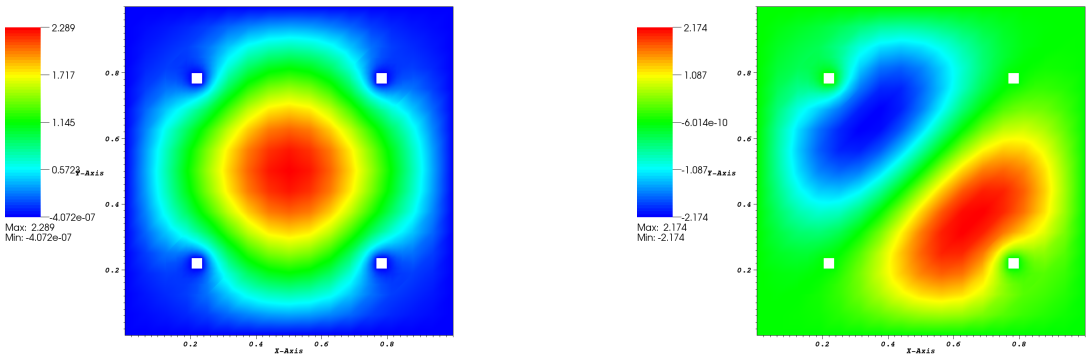

(a) (b)

Figure 4: Example 1: (a) Eigenfunction corresponding to the first eigenvalue. (b) Eigenfunction corresponding to the second eigenvalue.

In order to assess the quality of the computed DGCFEM solution on adaptively refined composite meshes, in Figure 5 we present the *hp*-adapted meshes for the first eigenvalue after 13 and after 25 iterations of the algorithm. As can you see after 13 iterations, the mesh is still quite coarse, even if the error is already quite small, and the method has not started yet to refine around the holes. On the other hand, after 25 iterations, the mesh very refined around the holes, especially around the corners of the holes, suggesting that we are in presence of lack of regularity in those regions. As suspected, in order to obtain very accurate approximation of the eigenvalue, at some point the method reach the scale of the small details.

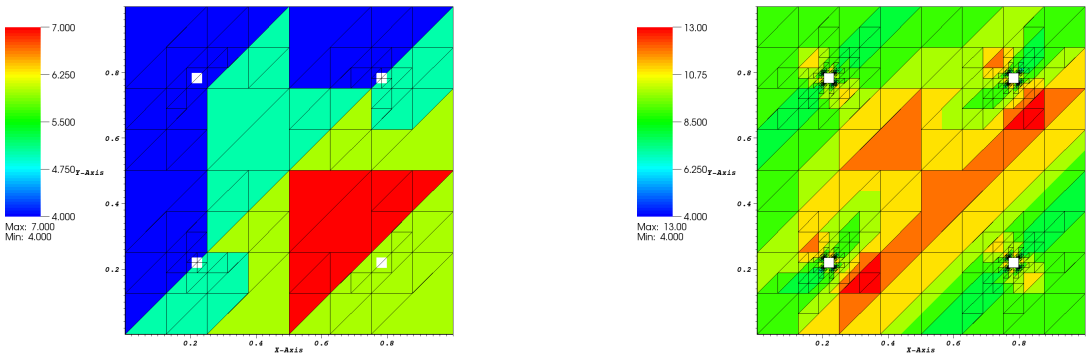

(a) (b)

Figure 5: Example 1: (a) *hp*-adapted mesh after 13 iterations of the adaptive procedure for the first eigenvalue. (b) *hp*-adapted mesh after 25 iterations of the adaptive procedure for the same eigenvalue. The color scheme indicate the order of polynomials used in each element.

In Figure 6 we present the *hp*-adapted meshes for the second eigenvalue after 17 and after 21 iterations of the algorithm respectively for the second and third eigenvalue. At closer inspection, the mesh in Figure 6(a) is not refined equally around all the corners of the small square holes. The method seems to be able to distinguish between those corners where singularities in the gradient arise due to the shape of the correspondent eigenfunctions, from those that do not play any active role for such eigenfunction.

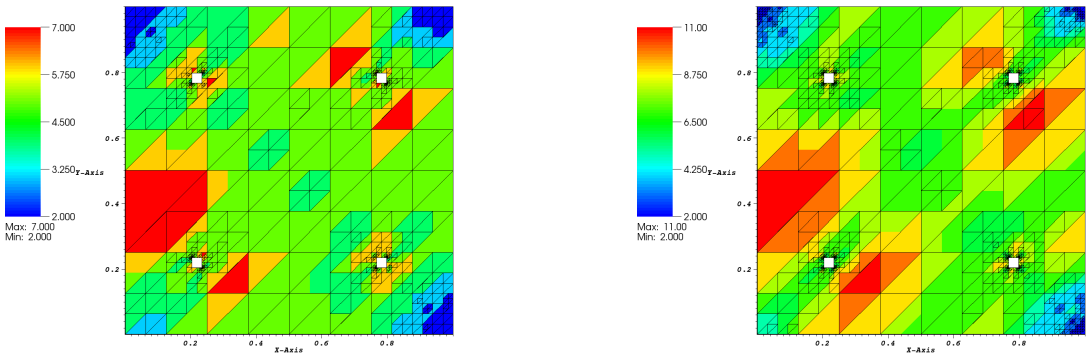

(a) (b)

Figure 6: Example 1: (a) *hp*-adapted mesh after 17 iterations of the adaptive procedure for the second eigenvalue. (b) *hp*-adapted mesh after 21 iterations of the adaptive procedure for the third eigenvalue. The color scheme indicate the order of polynomials used in each element.

5.2 Example 2: Random holes

In this second example, we consider a unit square domain with a series of square holes of size 1/32 placed randomly, see Figure 7. Our interest in this case is due to the fact that this kind of configuration is not covered by other methods like homogenization. The initial coarse mesh contains only 8 triangles and the initial value of $p = 2$ for all elements.

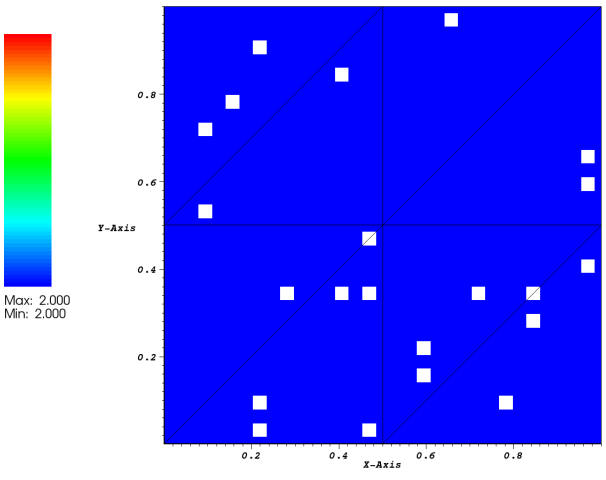

Figure 7: Example 2: Initial coarse mesh for the domain with randomly placed holes. The color scheme indicate the order of polynomials used in each element.

In Figures 8 and 9, we present the decay of the error for the first four eigenvalues and the corresponding error estimators. As can be seen, also in this case, the convergence for all eigenvalues look asymptotically exponential and the error estimator $\sum_{\kappa\in\mathcal{T}_{\mathtt{CFE}}}\eta_\kappa^2$ follows well the error. In Figures 10 and 11, we reported the values of the efficiency index for all the considered eigenvalues.

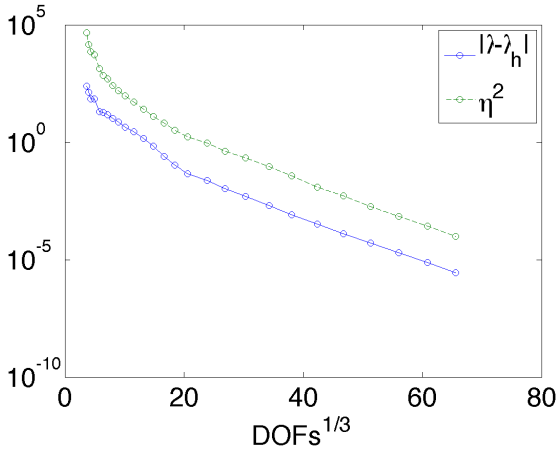

(a)

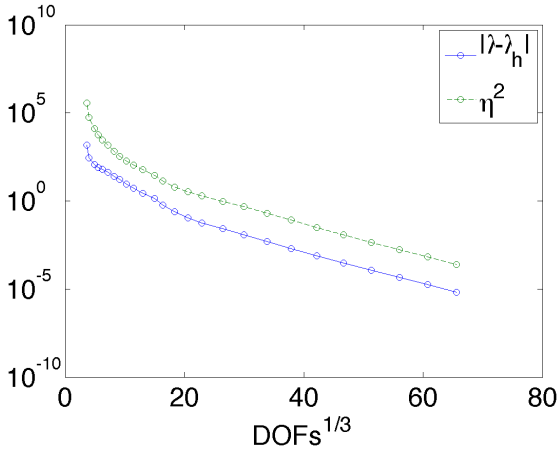

(b)

Figure 8: Example 2: (a) Convergence of the error for the first eigenvalue and of the corresponding error estimator. (b) Convergence of the error for the second eigenvalue and of the corresponding error estimator.

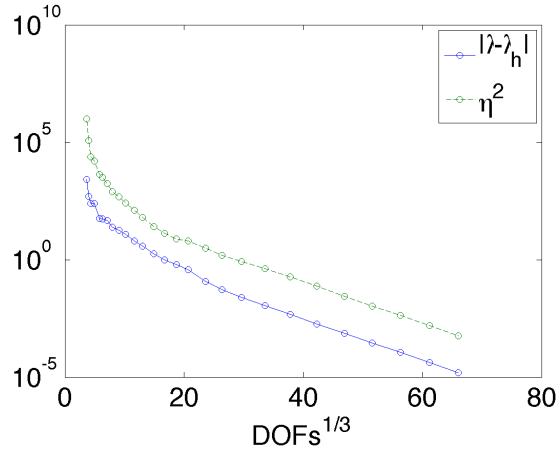

(a)

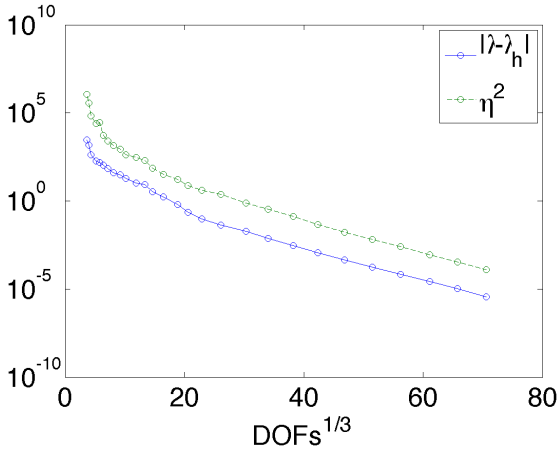

(b)

Figure 9: Example 2: (a) Convergence of the error for the third eigenvalue and of the corresponding error estimator. (b) Convergence of the error for the fourth eigenvalue and of the corresponding error estimator.

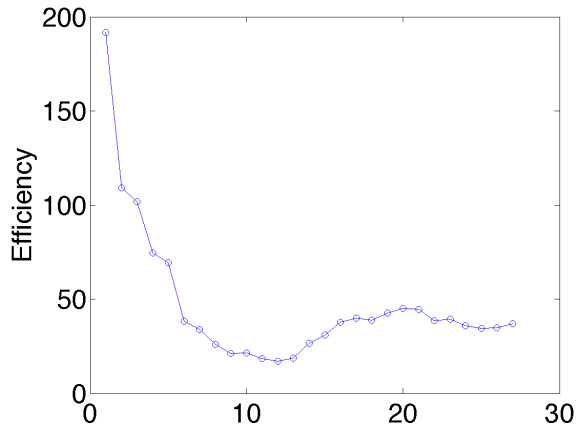

(a)

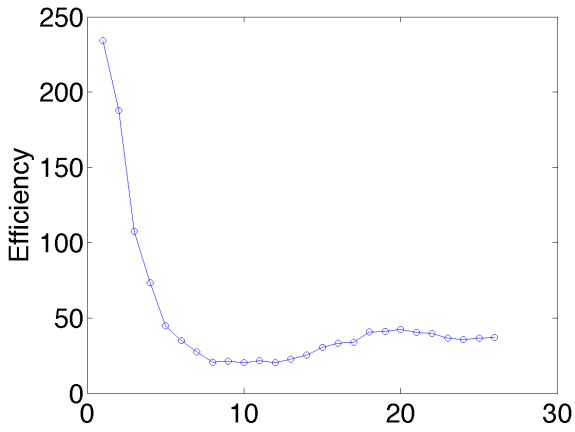

(b)

Figure 10: Example 2: (a) Efficiency index for the first eigenvalue. (b) Efficiency index for the second eigenvalue.

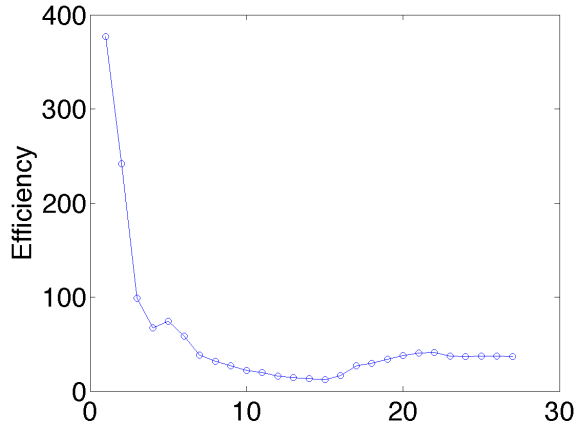

(a)

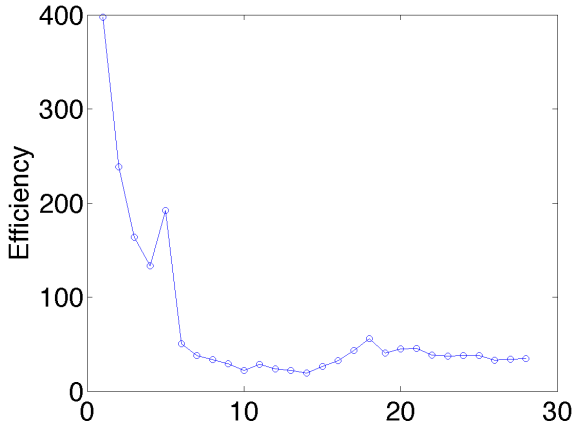

(b)

Figure 11: Example 2: (a) Efficiency index for the third eigenvalue. (b) Efficiency index for the fourth eigenvalue.

To have an idea of the shape of the eigenfunctions for this problem, in

Figures 12 and 13 we reported the pictures of eigenfunctions corresponding to the first four eigenvalues.

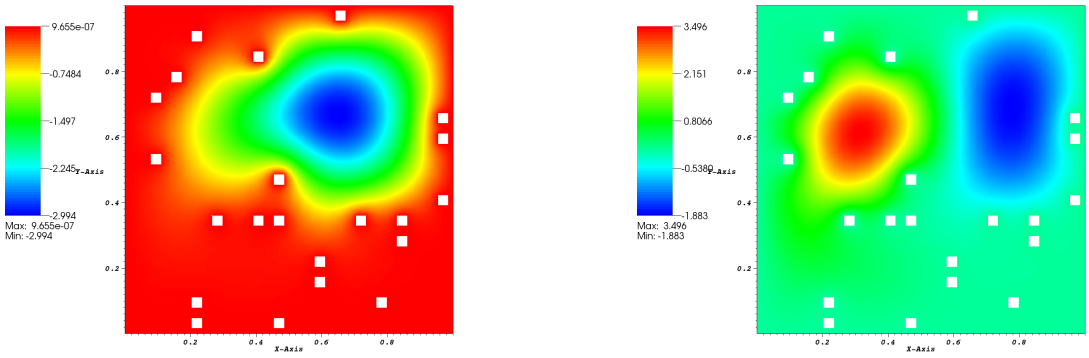

(a) (b)

Figure 12: Example 2: (a) Eigenfunction corresponding to the first eigenvalue. (b) Eigenfunction corresponding to the second eigenvalue.

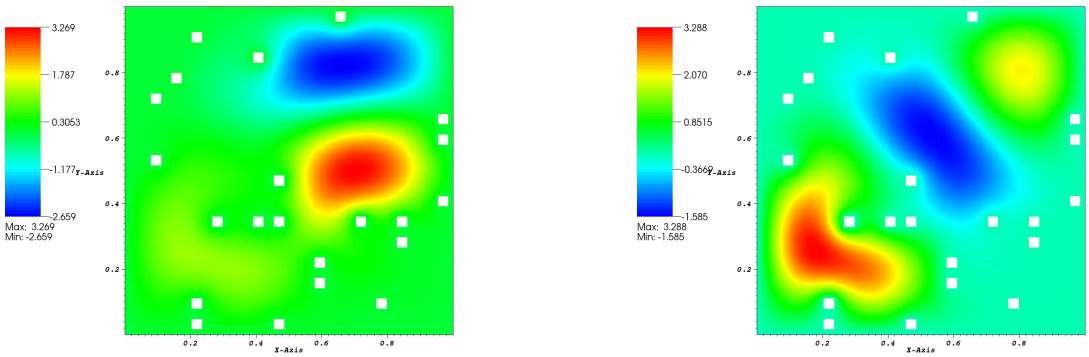

(a) (b)

Figure 13: Example 2: (a) Eigenfunction corresponding to the third eigenvalue. (b) Eigenfunction corresponding to the fourth eigenvalue.

In order to assess the quality of the computed DGCFEM solution on

adaptively refined composite meshes, in Figure 14 we present the *hp*-adapted meshes for the first eigenvalue after 17 and after 26 iterations of the algorithm. As before, the first mesh is still quite coarse, even if the error is already quite small, and in particular the method has not started yet to refine around the holes. On the other hand, after 26 iterations, the mesh very refined around the holes, especially around the corners of the holes, suggesting that we are in presence of lack of regularity in those regions.

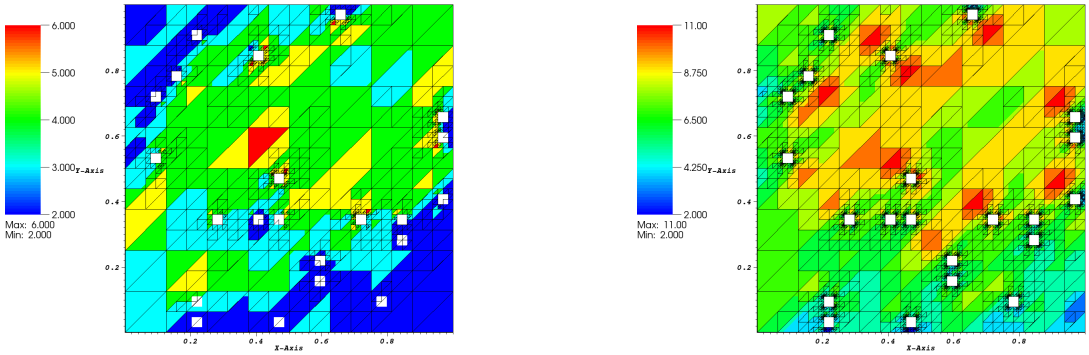

(a) (b)

Figure 14: Example 2: (a) *hp*-adapted mesh after 17 iterations of the adaptive procedure for the first eigenvalue. (b) *hp*-adapted mesh after 26 iterations of the adaptive procedure for the same eigenvalue. The color scheme indicate the order of polynomials used in each element.

The same conclusions can also been drawn from Figures 15, 16 and 17.

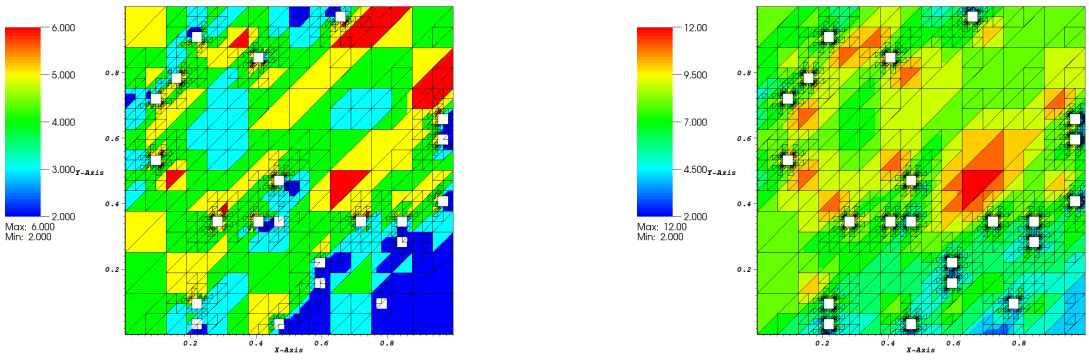

(a) (b)

Figure 15: Example 2: (a) *hp*-adapted mesh after 17 iterations of the adaptive procedure for the second eigenvalue. (b) *hp*-adapted mesh after 24 iterations of the adaptive procedure for the same eigenvalue. The color scheme indicate the order of polynomials used in each element.

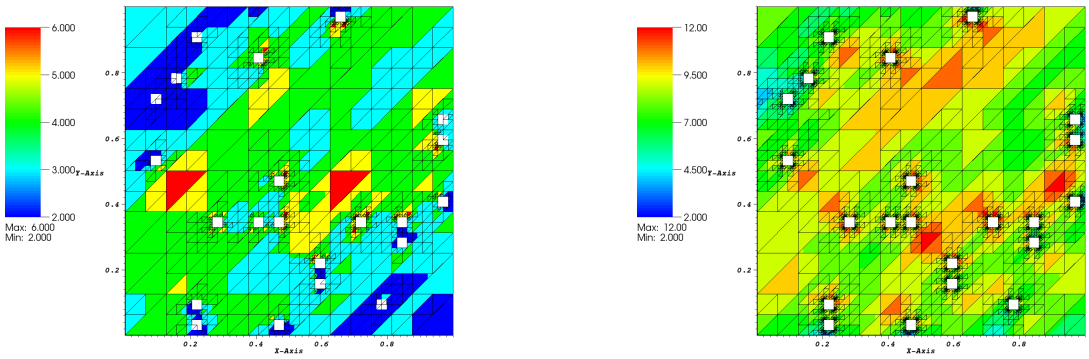

(a) (b)

Figure 16: Example 2: (a) *hp*-adapted mesh after 17 iterations of the adaptive procedure for the third eigenvalue. (b) *hp*-adapted mesh after 26 iterations of the adaptive procedure for the same eigenvalue. The color scheme indicate the order of polynomials used in each element.

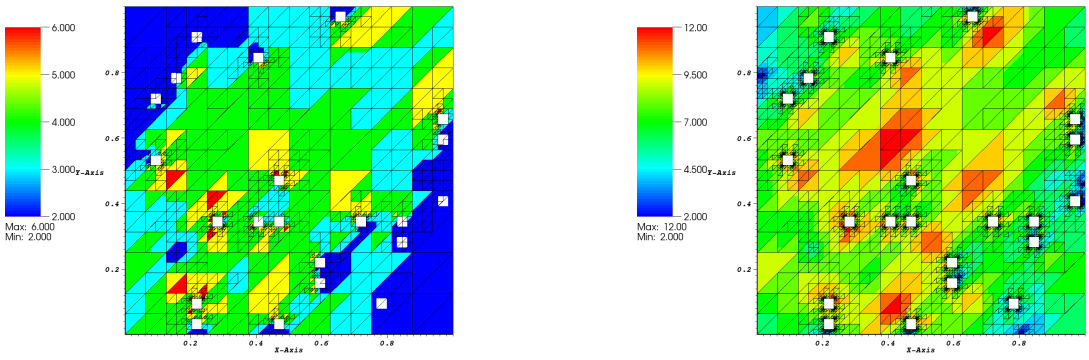

(a) (b)

Figure 17: Example 2: (a) *hp*-adapted mesh after 17 iterations of the adaptive procedure for the fourth eigenvalue. (b) *hp*-adapted mesh after 26 iterations of the adaptive procedure for the same eigenvalue. The color scheme indicate the order of polynomials used in each element.

6 Concluding remarks

In this article we have derived an energy norm *hp*–a posteriori error bound for the composite version of the discontinuous Galerkin discretization of second–order elliptic eigenvalue problems. This class of schemes naturally allows for the approximation of problems posed on so-called complicated domains using relatively coarse finite element spaces. Also this class of scheme is suitable for problems with non-periodic distributions of small features, which are not covered by other methods. The error estimator seems to be robust and the eigenvalues can approximated with very high accuracy for all configurations. From a practical point of view, the method is capable to deliver engineering accuracy on meshes too coarse to describe all the features of the domains and with a number of DOFs independent from the number of holes. Future work will be devoted to the consideration of more complex eigenvalue problems.

References

[1] P. Antonietti, S. Giani, P. Houston, *hp*–Version composite discontinuous Galerkin methods for elliptic problems on complicated domains, SIAM J. Sci. Comput. 35 (3) (2013) A1417–A1439.

[2] S. Giani, P. Houston, hp-adaptive composite discontinuous galerkin methods for elliptic problems on complicated domains, Numerical Methods for Partial Differential Equations (accepted).

[3] W. Hackbusch, S. Sauter, Composite finite elements for the approximation of PDEs on domains with complicated micro-structures, Numer. Math. 75 (1997) 447–472.

[4] W. Hackbusch, S. Sauter, Composite finite elements for problems containing small geometric details. Part II: Implementation and numerical results, Comput. Visual Sci. 1 (1997) 15–25.

[5] M. Rech, S. Sauter, A. Smolianski, Two-scale composite finite element method for the Dirichlet problem on complicated domains, Numer. Math. 102 (4) (2006) 681–708.

[6] P. Houston, D. Schötzau, T. Wihler, Energy norm a posteriori error estimation for mixed discontinuous Galerkin approximations of the Stokes problem, J. Sci. Comput. 22(1) (2005) 357–380.

[7] P. Houston, D. Schötzau, T. P. Wihler, An *hp*-adaptive mixed discontinuous Galerkin FEM for nearly incompressible linear elasticity, Comput. Methods Appl. Mech. Engrg. 195 (25-28) (2006) 3224–3246.

[8] P. Houston, D. Schötzau, T. P. Wihler, Energy norm a posteriori error estimation of *hp*-adaptive discontinuous Galerkin methods for elliptic problems, Math. Models Methods Appl. Sci. 17 (1) (2007) 33–62.

[9] P. Houston, E. Süli, T. Wihler, A posteriori error analysis of *hp*-version discontinuous Galerkin finite-element methods for second-order quasilinear PDEs, IMA J. Numer. Anal. 28 (2) (2007) 245–273.

[10] S. Kesavan, Homogenization of elliptic eigenvalue problem. part i, Appl. Math. Optim. (5) (1979) 153–167.

[11] S. Kesavan, Homogenization of elliptic eigenvalue problem. part ii, Appl. Math. Optim. (5) (1979) 197–216.

[12] G. Allaire, C. Conca, Bloch wave homogenization and spectral asymptotic analysis, Journal de Mathmatiques Pures et Appliques 77 (2) (1998) 153–208. doi:10.1016/S0021-7824(98)80068-8.
URL http://www.sciencedirect.com/science/article/pii/S0021782498800688

[13] M. Vanninathan, Homogenization of eigenvalue problems in perforated domains, Proceedings of the Indian Academy of Sciences - Mathematical Sciences 90 (3) (1981) 239–271. doi:10.1007/BF02838079.
URL http://link.springer.com/article/10.1007/BF02838079

[14] J. Nolen, G. Papanicolaou, O. Pironneau, A framework for adaptive multiscale methods for elliptic problems, Multiscale Modeling & Simulation 7 (1) (2008) 171–196. doi:10.1137/070693230.
URL http://epubs.siam.org/doi/abs/10.1137/070693230

[15] T. J. R. Hughes, G. R. Feijo, L. Mazzei, J.-B. Quincy, The variational multiscale methoda paradigm for computational mechanics, Computer Methods in Applied Mechanics and Engineering 166 (12) (1998) 3–24. doi:10.1016/S0045-7825(98)00079-6.
URL http://www.sciencedirect.com/science/article/pii/S0045782598000796

[16] T. Arbogast, Analysis of a two-scale, locally conservative subgrid upscaling for elliptic problems, SIAM Journal on Numerical Analysis 42 (2) (2004) 576–598. doi:10.1137/S0036142902406636.
URL http://epubs.siam.org/doi/abs/10.1137/S0036142902406636

[17] S. Giani, E. Hall, An a posteriori error estimator for hp-adaptive discontinuous galerkin methods for elliptic eigenvalue problems, Mathematical Models and Methods in Applied Sciences 22 (10) (2012) 1250030.

[18] S. Giani, I. G. Graham, Adaptive finite element methods for computing band gaps in photonic crystals, Numerische Mathematik (121) (2012) 31–64.

[19] D. Arnold, F. Brezzi, B. Cockburn, L. Marini, Unified analysis of discontinuous Galerkin methods for elliptic problems, SIAM J. Numer. Anal. 39 (2001) 1749–1779.

[20] L. Zhu, D. Schötzau, A robust a posteriori error estimate for *hp*–adaptive DG methods for convection-diffusion equations, IMA J. Numer. Anal. 31 (3) (2010) 971–1005.

[21] L. Zhu, S. Giani, P. Houston, D. Schötzau, Energy norm a posteriori error estimation for *hp*-adaptive discontinuous Galerkin methods for elliptic problems in three dimensions, Math. Model. Methods Appl. Sci. 21 (2) (2011) 267–306. doi:10.1142/S0218202511005052.

[22] R. Hartmann, Numerical analysis of higher order discontinuous Galerkin finite element methods, in: H. Deconinck (Ed.), VKI LS 2008-08: CFD - ADIGMA course on very high order discretization methods, Oct. 13-17, 2008, Von Karman Institute for Fluid Dynamics, Rhode Saint Genèse, Belgium, 2008.

[23] R. B. Lehoucq, D. C. Sorensen, C. Yang, ARPACK users' guide, Vol. 6 of Software, Environments, and Tools, Society for Industrial and Applied Mathematics (SIAM), Philadelphia, PA, 1998, solution of large-scale eigenvalue problems with implicitly restarted Arnoldi methods.

[24] P. R. Amestoy, I. S. Duff, J. Koster, J.-Y. L'Excellent, A fully asynchronous multifrontal solver using distributed dynamic scheduling, SIAM J. Matrix Anal. Appl. 23 (1) (2001) 15–41.

[25] P. R. Amestoy, I. S. Duff, J.-Y. L'Excellent, Multifrontal parallel distributed symmetricand unsymmetric solvers, Comput. Methods Appl. Mech. Eng. 184 (2000) 501–520.

[26] P. R. Amestoy, A. Guermouche, J.-Y. L'Excellent, S. Pralet, Hybrid scheduling for the parallel solution of linear systems, Parallel Computing 32 (2) (2006) 136–156.

[27] P. Houston, E. Süli, A note on the design of *hp*-adaptive finite element methods for elliptic partial differential equations, Comput. Methods Appl. Mech. Engrg. 194 (2–5) (2005) 229–243. doi:10.1016/j.cma.2004.04.009.

[28] T. Eibner, J. Melenk, An adaptive strategy for hp-FEM based on testing for analyticity, Comp. Mech. 39 (2007) 575–595.

[29] T. Wihler, An *hp*-adaptive strategy based on continuous Sobolev embedding, J. Comput. Appl. Math. 235 (2011) 2731–2739.

[30] W. Mitchell, M. McClain, A comparison of *hp*–adaptive strategies for elliptic partial differential equations, Submitted for publication.